



TIP VORTEX DEVELOPMENT AND STRUCTURE AT BVI FOR A HOVERING ROTOR  
WITH SWEEPED BACK TIP SHAPES USING THE FLOW VISUALIZATION GUN TECHNIQUE

BY

R. H. G. MÜLLER

F.I.B.U.S. RESEARCH INSTITUTE  
PAUL-KLEE-WEG 8  
D-40217 DÜSSELDORF, GERMANY

AND

D.FAVIER, M. NSI MBA, E. BERTON, C. MARESCA

INSTITUT DE MECANIQUE DES FLUIDES  
UNIVERSITE D'AIX MARSEILLE II, UM-34 DU C.N.R.S.  
SUFFLERIES DE LUMINY, 163 AVENUE DE LUMINY, 13009 MARSEILLE, FRANCE

**TWENTIETH EUROPEAN ROTORCRAFT FORUM**  
**OCTOBER 4 - 7, 1994 AMSTERDAM**

# Tip Vortex Development and Structure at BVI for a Hovering Rotor with Swept Back Tip Shapes Using the Flow Visualization Gun Technique

by

R. H. G. Müller  
F.I.B.U.S. Research Institute  
Paul-Klee-Weg 8  
D-40489 Düsseldorf, Germany

and

D. Favier, M. Nsi Mba, E. Berton, C. Maresca  
Institut de Mécanique des Fluides  
Université d'Aix-Marseille II, UM-34 du C.N.R.S.  
Suffleries de Luminy, 163 avenue de Luminy, 13009 Marseille, France

## ABSTRACT

The objective of this associated research project was to apply a novel smoke visualization technique (the "Flow Visualization Gun" technique) to the helicopter rotor flow at the Institut de Mécanique des Fluides in Marseille (IMFM). At the IMFM, the rotor flow of several different rotor types has been investigated thoroughly using the Laser Doppler Anemometry technique (LDA). Whereas the LDA is a point-based Eulerian Method, the new visualization technique provides a Lagrangian view of the flow. Using "time lines", i.e. smoke lines which are placed into the flow instantaneously and which follow the local flow accurately, flow pattern development and flow distortion over space and time can be observed and photographed. Extensive qualitative information on complex flow patterns like rolled-up vortices can be obtained by interpretation of the photographs. While other visualization techniques like the smoke filament injection showed diffuse streamlines and the locations of the vortex cores only, the novel technique allows even quantitative measurements of the flow velocities. Besides of the presentation of some highlight visualization photographs of rotor blade tip vortices and rotor downwash, the procedure to obtain quantitative velocity data sets of the flow using stereometric photographs and digital image processing techniques will be outlined. Using a 3-dimensional weighted interpolation procedure, velocity vector plots and vorticity plots have been produced which are compared to the grid based data sets of the Laser velocimetry. A good agreement between the different techniques validates the novel FVG technique as a perfect tool to provide qualitative information of complex unsteady flow patterns and at the same time quantitative data on the flow velocities.

## 1. INTRODUCTION

Blade Vortex Interaction noise (BVI) or dynamic blade loads are important factors in the design of helicopter rotors. Calculations, using Biot-Savart law or even CFD codes, still cannot reflect the pressure fluctuations on the blade surface during a vortex encounter accurately. Normally, they overpredict the pressure peaks. Reason for this uncertainty is the fact that the vortex structure and its development due to the strong influence of the pressure field of the approaching blade are not very well understood. This understanding, however, is absolutely necessary if new types of blade tip geometries have to be investigated. The application of new experimental techniques will provide this essential information. Among these techniques, especially the flow visualization techniques are important tools for the study of complex flow patterns. The visualization images allow the qualitative description of the entire flow field and, in some cases, also the quantitative measurement of flow characteristics like vortex core location or even the flow velocities. It is very important to obtain these quantitative data for the verification of flow field calculations using Computational Fluid Dynamics codes (CFD).

An associated project between the Institut de Mécanique des Fluides in Marseille (IMFM) and the F.I.B.U.S. research institute has been initiated. The main objective of this joint project is the investigation of the applicability of different measurement techniques to the complex rotor flow and to provide data and information for a better physical understanding of this special flow. The Laser velocimetry (Laser Doppler Anemometry LDA), which has been used at the IMFM for many years, provides very accurate measurements of the flow velocities and the bound circulation on the blade. However, it is a point based Eulerian method: It measures one point at a time. To obtain a large data set, the data of many rotor revolutions have to be combined. Due to the fact that the formation of the tip vortex at the blade tip or the development of the older tip vortex at BVI with the following blade are unsteady flow patterns even in hover flight, their investigation using LDA is not possible or at least strongly restricted. Only

the mean velocities of these flow types can be measured.

On the other hand, a flow visualization technique like the novel "Flow Visualization Gun" technique can depict a distinct flow pattern of relatively large spatial dimension in one single picture at one single very short time interval. A huge amount of information on the interesting flow pattern can be obtained by interpretation of this single flow picture. Due to the Lagrangian view of this visualization the development of a distinct flow pattern can be followed and interpreted. This is very helpful for the physical understanding of the flow. Additionally to this qualitative and quantitative information on unique and distinctive flow patterns, the new technique can also be used to produce large spatial data sets which can directly be compared to the data sets of the Laser velocimetry. This can be achieved by combination of the information of many flow photographs by a 3-dimensional interpolation in space and time. Then, of course, we have the same restrictions like the LDA technique.

Currently used visualization methods, like smoke injection, smoke wire, pulsed smoke wire, the helium bubble technique, the spark tracer technique, or the phosphorescent tracer techniques all have distinct disadvantages which prevent their application to special flow fields like the helicopter rotor flow. A more detailed discussion and comparison of these methods is presented in refs. 2, 3 and 4. In this report, the "Flow Visualization Gun"-technique and its application to complex helicopter rotor flows will be presented. This novel technique has been initiated by Steinhoff (ref. 1). The development of this technique for the application to complex rotor flow has been performed by the author at the University of Tennessee Space Institute (ref. 2, 3). The technique has several advantages over the currently used visualization methods. After a short principal description of the technique (a more detailed description can be found in refs. 2, 3 and 4), several flow photographs will be presented and discussed, emphasizing the advantages of the new method for the investigation of complex flow fields like the rotor flow containing developing tip vortices and blade vortex interactions.

Quantitative results, obtained by using digital image analysis techniques (ref. 4), will be presented including plots of the tip vortex structure and the downwash in the tip region of the test rotor. LDA measurements of the same rotor configuration have been performed. The results will be used for comparison and validation of the data produced by the visualization.

## 2. THE NEW VISUALIZATION TECHNIQUE

The novel "Flow Visualization Gun"-technique (FVG) is based on the idea to produce, at one instant, an initially straight line of smoke within the flow at an arbitrary direction or location, normally perpendicular to the main flow. The smoke particles in this smoke trace are very small and follow the airflow very accurately. Their motion can be used to determine the flow velocities normal to the smoke trace and, under certain circumstances, also along the trace. The smoke traces have sharp edges, are very thin, can cover distances greater than one meter, and can be placed almost everywhere in the flow field, even intersecting the rotor disc. They are created by heating very small titanium pellets and projecting them through the flow at high speed. Due to the heating process the pellets are burning and produce a trace of dense, white titanium dioxide smoke in their wake. As such a pellet has a diameter of less than 0.1 millimeter, its wake and therefore the smoke trace is not wider than 0.5 millimeter. The disturbance of the flow induced by the pellet and its wake is apparently very small and can be neglected, since when the trace is being observed, the pellet has gone beyond the region of observation a distance of several orders of magnitude greater than its diameter and all disturbances in the wake have decayed. After being placed into the flow, the smoke trace behaves like a "time line". Using a stroboscope or several triggered flashes, the light scattered by the smoke can be photographed. Flow velocities can be determined by measuring the displacement of the smoke trace images at subsequent flashes on a single photograph.

The shooting mechanism consists of a thin glass pipette and works according to the principle of an exploding wire (ref. 7 to 9) (see figure 1). A relatively large (1 millimeter diameter) titanium pellet electrically connects two wires.

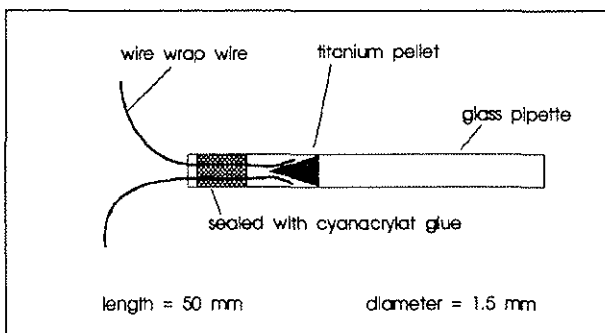


Fig. 1 Shooting element for titanium particles

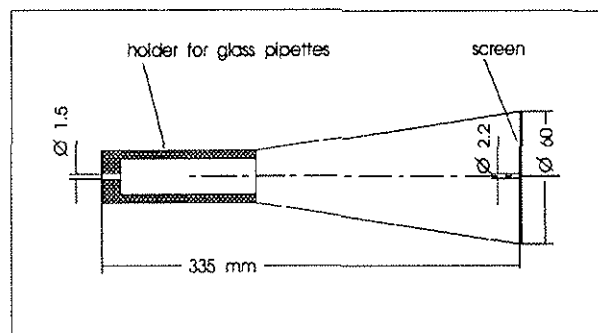


Fig. 2 Flow Visualization Gun - holder for shooting elements

Power is supplied by large capacitors (250 Volt at 1000 microFarads). In a strong wire explosion the relatively large titanium pellet partially disintegrates into extremely small particles, which start burning. These particles have a diameter of less than 0.1 mm. The rest of the large pellet, which is of no further interest, and all the burning particles are accelerated by the explosion and leave the glass pipette like the shot of a shotgun at a spreading angle of approximately 5 degree and at a speed of 200m/s and more, depending on the energy provided by the capacitors. At the distance of 0.3 m a screen (figure 2) with a small hole extracts one of these small particles, which then finally continues along its path through the region of interest of the flow. Due to this special screen arrangement, the probability is high that only one particle leaves the apparatus and produces one single smoke trace (If more than one particle leave the gun, the photographs will be crowded with smoke lines and the interpretation will be more difficult). Due to the aerodynamic drag, the final particle speed after passing the screen has lowered to something between 50m/s and 80m/s. For longer shooting ranges, the particle speed will slow down even further.

Usable shooting distance with the gun is about 0.5 m to 1.0 m, depending on the particle speed, size, and temperature. After this distance, the particle becomes thermally unstable and disintegrates into a firework of even smaller particles, which produce no smoke.

When the particle has crossed the whole region of interest, the smoke trace is ready to be photographed. At this time, however, the trace is already influenced by the flow and by flow disturbances. This means that the older parts of the smoke trace may have irregularities. This effect, rather than causing a problem, is helpful for determining the flow velocities even in direction of the smoke line itself by following distinct recognizable local irregularities over subsequent flashes.

For the illumination of the smoke traces a set of up to four pre-charged flashes has been used, because a regular stroboscope can not produce high energy flashes (20Ws) at the necessary high frequency of up to 2000Hz for the relatively high speed flow. Flash rising time is 0.01ms and decay time to half intensity is about 0.5ms. Due to this relatively long decay time, the "leading edge" of the smoke trace image, i.e., the edge in the direction of the flow velocity, is fading out diffusely. The trailing edge (this is the position of the line at the flash rise), however, is very sharp due to the very fast flash rising time. Therefore, just the sharp trailing edge should be used for velocity measurements. Since there is one sharp edge, the relatively large width of the line image has no adverse effect. On the contrary, it can be helpful to determine the flow direction by observation of the direction of the fading out of the smoke trace image.

For taking photographs, the camera shutter normally stays open from the time of the explosion till the end of the flash sequence. Since the particle is incandescent, it leaves a photographic image as it traverses the flow, separate from and additional to the illuminated smoke trace images. Due to drag forces on the particle caused by the airflow, its path and therefore its image in the photograph is not exactly a straight line. This effect can be large at high cross flow velocities and influences the location of the smoke trace. It is therefore not possible to place the line at an exactly predefined position.

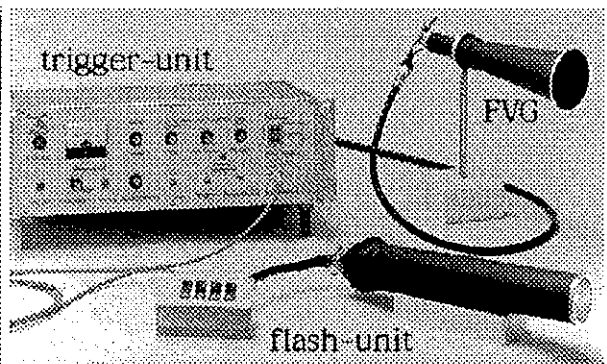
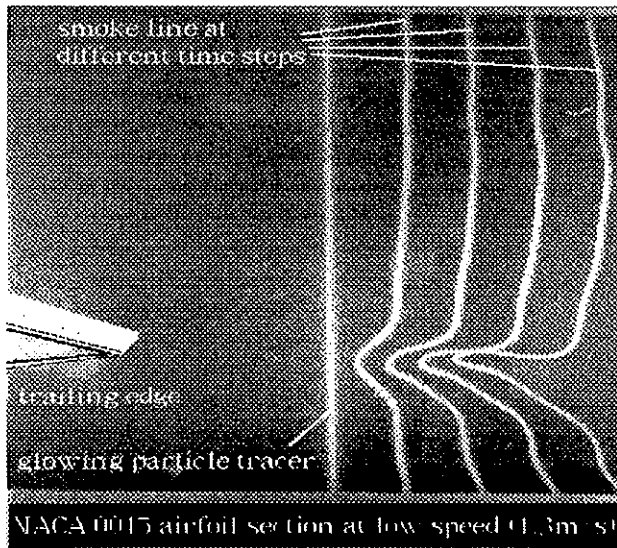


Fig. 4 Flow Visualization Gun Apparatus

Fig. 3 Wake defect behind an airfoil section

An example and first impression of the capabilities of the method is presented in figure 3 in an initial non-rotor test. Here, in a simple environment, the wake of an airfoil section in a small windtunnel at a very low air speed of 1.3 m/s is shown. The straight line is the image of the incandescent titanium particle crossing the flow region. In a four-flash-sequence the smoke line shows the flow in the wake of the airfoil. The wake defect behind the trailing edge of the airfoil can be observed very clearly. In all the following smoke photographs the gray levels will be inverted, giving black smoke lines on white background. This technique greatly enhances the visibility of the faint lines at higher flow speeds.

The "Flow Visualization Gun" technique is used by applying the FVG apparatus, which has been developed by the F.I.B.U.S. research institute. It consists of the "trigger-unit", the "flash-unit" and the "Flow Visualization Gun" itself which holds the "shooting elements" (figure 4). The "trigger-unit" provides the electrical power to drive the titanium particle explosion and the flash sequence and produces all trigger signals to synchronize with the rotating rotor. The "flash unit" is a special flash device, equipped with four single flashes in a combined optical arrangement, which can be fired at very short time intervals, ranging from 10 ms down to 0.1 ms.

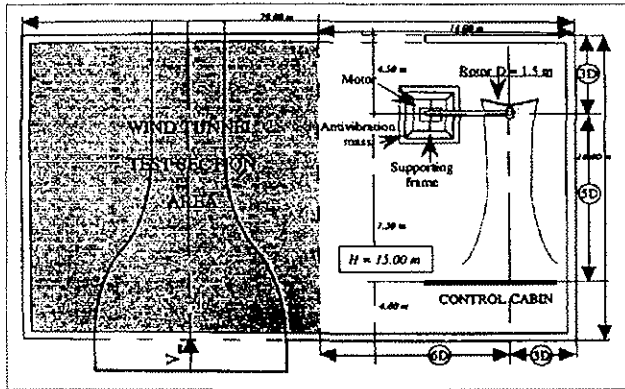


Fig. 5 Rotor set up in the windtunnel hall

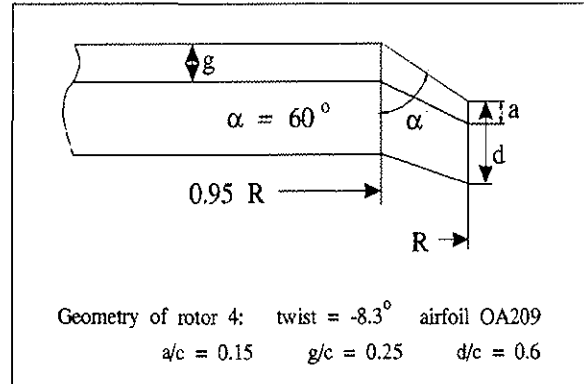


Fig. 6 Geometry of rotor no 4

### 3. THE TEST ROTOR AND THE EXPERIMENTAL SET UP

The rotor system used for the experiments is set up on the hovering test rig installed in the large testing hall of the S1-Luminy wind tunnel (figure 5). Distance to the walls is expressed in terms of rotor diameters in figure 5. The rotor consists of a fully articulated rotor hub which can be equipped with different sets of blades. The blade set No 4 has been used to perform the experiments discussed throughout this report. These blades have a swept back tip shape (figure 6). Data of this rotor are given in the following table (see also refs. 11, 12):

radius	0.75m
rotational speed	683min <sup>-1</sup> (and for some tests 1365min <sup>-1</sup> )
tip speed	53.5m/s (and for some tests 107m/s)
chord	0.05m
root cutout	0.22 radius
coning angle	2.5 degree
airfoil	OA209
blade shape	rectangular with a 60 degree swept back tip
number of blades	2 blades (and for some tests 4 blades)
twist	-8.3 degree
angle of attack	10 degree at 0.75 radius

Table 1: Rotor No 4 of the IMFM

timing between subsequent flashes:

Fig. 7, 8, 9:	0.5 ms
Fig. 10, 11:	1.0 ms
Fig. 12:	0.8 ms
Fig. 13, 14:	0.5 ms
Fig. 15:	0.4 ms

Table 2: Flash timing

Two different tip speeds were used during the experiments. The regular tip speed used for most earlier tests at IMFM (especially the Laser velocimetry) is 107m/s. As the new visualization technique had not been verified for this relatively high tip speed, the half speed (53.5m/s tip speed) has been used for most of the visualization experiments. As can be seen in some of the test photographs for full speed, however, this is not the limit for the method: even at the full tip speed of 107m/s the smoke lines are visible and measurements are possible (figure 14, 15). However, a higher power of the flash light source should be provided to give an even better visibility of the smoke lines at the resulting high flow velocities under all experimental conditions.

In the 4-bladed configuration, the tip vortex of the preceding blade has a very close encounter with the rotor blade (figure 13). This phenomenon is called Blade Vortex Interaction (BVI) and causes large unsteady loads on the blade near the tip. In the 2-bladed configuration, the vertical spacing between the tip vortex and the following rotor blade at BVI is much larger due to the larger spacing between the two blades of 180 degrees. As one of the objectives of the experiments was the collection of information on the flow induced by the special swept back tip shape of the rotor No 4, the 2-bladed configuration was used for most of the experiments. It was assumed that this configuration would provide the possibility to separate the influences of swept tip shape and BVI more easily.

Two cameras were used simultaneously to provide a stereometric view of the smoke line images. One of these (the "tangential view camera") was set to have a tangential view of the rotor, looking at the blade trailing edge and showing the radial and axial flow of the downwash near the blade and the tangential velocities in the tip vortices. The other camera was set perpendicular to the "tangential view camera", depending on the experimental configuration, i. e. of the setting of the Flow Visualization Gun. When shooting the titanium particle perpendicular to the rotor disc, the camera was set to have a radial view towards the tip of the rotor blade, showing the chordwise flow near the blade. When shooting the particle radially inward toward the rotor head, the camera was set to have a view parallel to the rotor axis. Here it had a view on the radial and tangential flow of the downwash.

A very high sensitive KODAK TMAX P 3200 film was pushed to 25,000 ASA. The cameras used were an OLYMPUS OM-2 with a 100mm lens at an F-stop of 2.8 or 4.0 and a CANON F-1 with a 135mm lens at an F-stop of 3.5. The opening of the manual camera shutter was used to start the complete experimental sequence, while the azimuthal rotor blade position was used to trigger the shot of the titanium particle and the flash sequence at the right timing.

All laser velocimetry data were produced using the 2.5 W fiber optics laser (type COHERENT Innova 300) of the IMFM. It is a single component system. Axial, radial, and tangential velocities were not acquired concurrently. Use of a 500 step encoder afforded an azimuthal resolution of 0.72 degree (approximately 0.15 chords at 0.75R). The resolution in radial and axial direction was 2 cm. Due to this relatively coarse resolution the comparison to the flow visualization data is restricted to overall velocity comparisons. The small scale vortex structure, which can not be measured with this coarse grid will be topic of more thorough investigations in the future. For more information on the laser velocimetry see ref. 11 and 12.

#### 4. ACCURACY OF THE FVG-TECHNIQUE USING DIGITAL IMAGE ANALYSIS

The FVG-technique itself has a very high accuracy. The smoke particles can be considered to follow these low speed flow types very accurately, because the size of the smoke particles is less than 1 micron. For a general discussion of the possible errors in the velocity determination using time lines see ref. 10. The resolution of the technique for flow velocity measurement depends on the fine grain of the photographic film material and on the technique how to determine the edge of the smoke line images in the photographs. For using digital image analysis techniques for the velocity determination, the images have to be transferred into arrays of picture elements (pixel) by a video camera and a "frame grabber". This is a digitization hardware which converts the analog gray level image into 2-dimensional pixel arrays of 8 bits or 256 gray levels from black to white. This digitization process normally limits the image resolution to the size of one pixel. Regular video cameras used for this digitization have a resolution of 768 \* 512 pixels. However, the final resolution of the digitized image depends on the electronics and the optics of the camera and on the characteristics of the analog/digital-converter of the frame grabber. Normally, a maximum resolution of about 520 pixel horizontally and 400 pixel vertically can be achieved. From this value, knowing the translation factor between original photograph and pixel array, it is easy to determine the maximum spatial resolution. Using the time delay between two adjacent flashes, the minimum detectable velocity steps can be calculated. The minimum possible error is exactly half this velocity step. For the experiments discussed in this report, the minimum errors are between 0.15 and 0.3 m/s, depending on the flash timing between 0.5 and 1.0 ms. For the vortical regions with tangential velocities of 5 to 10 m/s and more this is a small error. For the tangential flow velocities of the rotor downwash apart from the vortices and the rotor blades which are in the order of 1.0 m/s this is a very large error. For real applications, the error will be at least double the minimum error, depending on the visibility of the smoke traces and on the detection of the smoke line edges which, of course, do not correspond to exact pixel boundaries.

If necessary, the accuracy can be increased very easily by using improved digitization equipment and procedures: by using a high resolution video camera of 1280 \* 1024 pixel or a film scanner, the accuracy can be increased by a factor of two and more. By using smaller regions of the flow for digitization, the resolution can again be increased. Here, we come already near to the resolution limit of the film material, which is relatively coarse due to the high light sensitivity. Finally, the resolution can be increased again by a factor of two or more by using "subpixel" algorithms. These are techniques to determine the edge of a line by the location of the maximum of the gray level gradient. This maximum gradient does not necessarily correspond exactly with pixel boundaries. All these improvements give a possible resolution of better than 0.1 m/s.

Using digital image processing, the computer can help to produce quantitative data of the velocity field. At the F.I.B.U.S. institute, a special software package has been developed - the picCOLOR 34 software - which allows the 3-dimensional vectorization and treatment of the smoke lines. Using the corresponding points (the earlier mentioned irregularities) on the smoke line images, the program calculates the mean local flow velocities between each two subsequent flashes. In the following steps of the procedure, the computer combines two stereometrically taken photographs to produce 3-dimensional data sets of the smoke line images. These data sets can be plotted as 3-

dimensional smoke line plots or as streamline plots. Even the complete velocity vector plot or the vorticity contour plot of a larger flow field can be calculated, using a larger set of stereometric photographs of that flow field. A special 3-dimensional, linear, spatial weighted interpolation procedure is used to provide the data on a regularly spaced grid. More details regarding the image processing and the 3-dimensional interpolation can be found in refs. 3, 4.

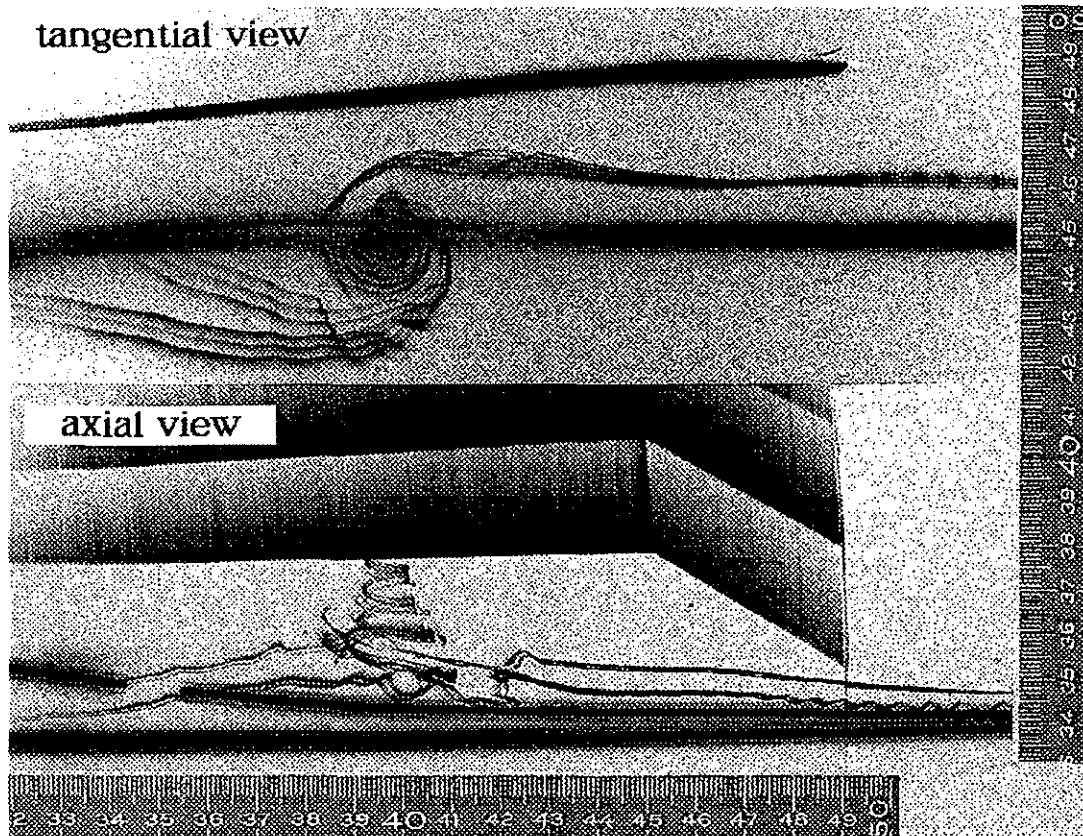


Fig. 7 Top: tangential view of the rotor flow, including vortex of preceding blade  
Bottom: axial view of the rotor flow (2 smoke lines, 3-flash-sequence)

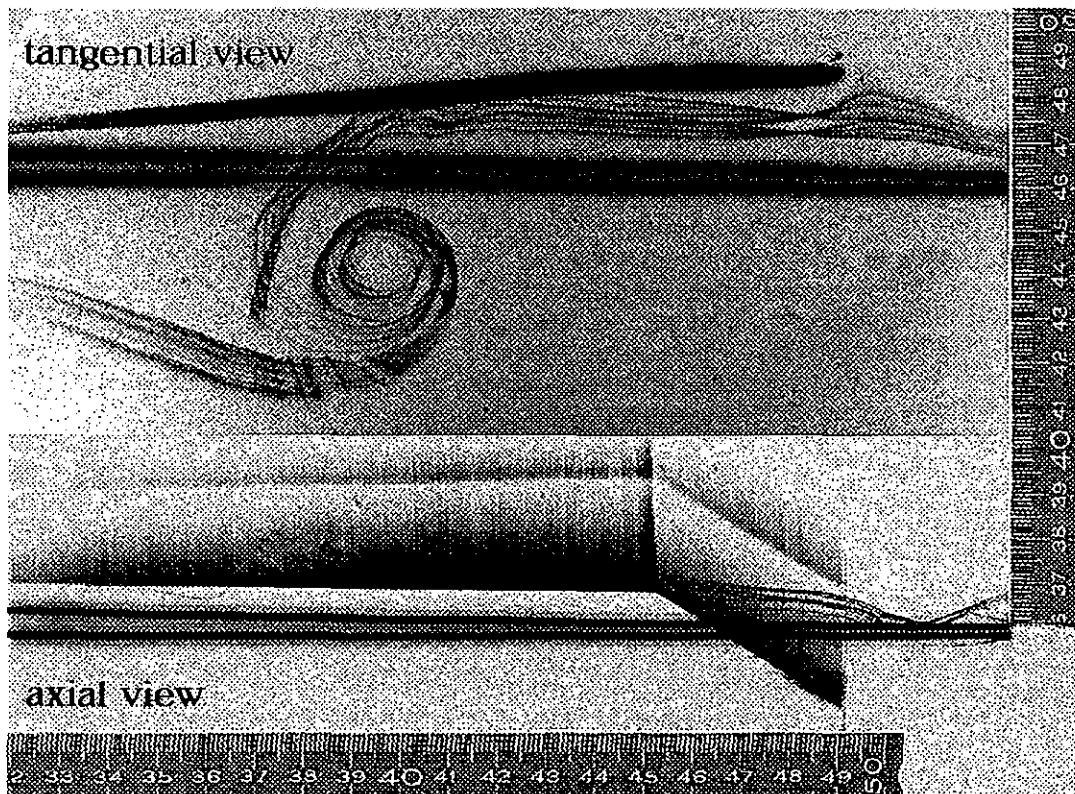


Fig. 8 Top: tangential view of the rotor flow. Bottom: axial view of the rotor flow. (2 smoke lines, 4 flashes)

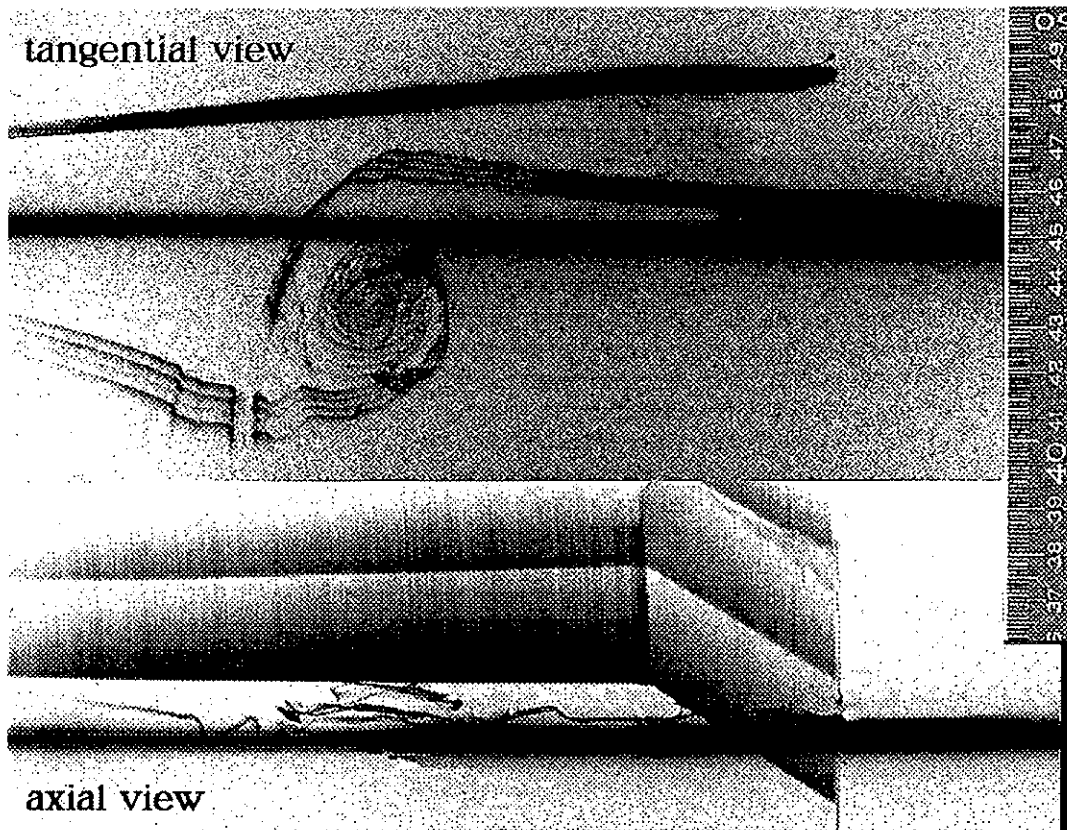


Fig. 9 Top: tangential view of the rotor flow; Bottom: axial view of the rotor flow (1 smoke line, 4 flashes)

## 5. DISCUSSION OF THE FLOW VISUALIZATION IMAGES

Figures 7 to 9 give impressive examples of the novel technique to visualize the rolled-up tip vortex of the test rotor at the interaction with the following rotor blade. From the two cameras we get the tangential view, showing the trailing edge of the blade (tip in the upper right hand corner) and the axial view, showing the illuminated leading edge of the blade at the subsequent flashes (see the leading edge shape of the swept back tip, moving upward in the photograph). We can see one or more traces of burning titanium particles and we see the images of the illuminated smoke lines at different time steps. For fig. 7, a three flash sequence was used, for the other figures four flashes were fired. Here, the blade hides the axial view of the vortex at the first flash.

Even after a roll-up of 5 or 6 revolutions the smoke lines are still connected and distinguishable. This gives evidence that the vortices have a very clean and laminar structure. Some little irregularities in the outer core of the vortices help to determine the tangential velocities in this region. Especially the lower side of figure 7 gives an excellent view on the axial flow in the vortex core. It is assumed that this is the first time that the complete structure of a tip vortex of a helicopter rotor during BVI has been visualized that clearly. To be able to measure the axial vortex velocity very accurately, more images have to be taken at different azimuthal positions relative to the rotor blade. As one objective of the experiments was to observe the influence of the blade tip shape on the wake, the flashes were triggered on the azimuthal blade position showing the flow at and directly behind the trailing edge. As mentioned before, however, in this configuration the blade normally hides the structure of the rolled-up vortex.

In figures 10 and 11 the particle has been shot perpendicular to the rotor disc. Additionally, the particle has been shot at a slightly later time than for the figures 7 to 9. As a result the vortex has not rolled up the line many times like in the figures 7 to 9. Photographs like these help to obtain information on the vortex structure and on the flow very near to the rotor blade and in its direct wake.

Figure 12 presents the developing tip vortex. On the left hand side we see the outer part of the tip vortex - no smoke has been placed into the core. On the right hand side the burning particle has been placed a little more inward. Here, the smoke line could be placed into the very core of the tip vortex. Due to the strong interaction with the blade the line has been separated and is influenced by the boundary layer of the blade. In these four flash sequences, the first flash was fired, when the blade had just passed the smoke line, i. e. the smoke line is at the trailing edge of the blade and the blade had exactly the time to cover one chord of distance to distort the smoke line and to roll it up into the freshly developing vortex. At the second flash the blade has moved almost one chord further and we can observe the roll up of the flow into the tip vortex. Following are the third and fourth of the flashes, with a vortex age of two or three chords, respectively.

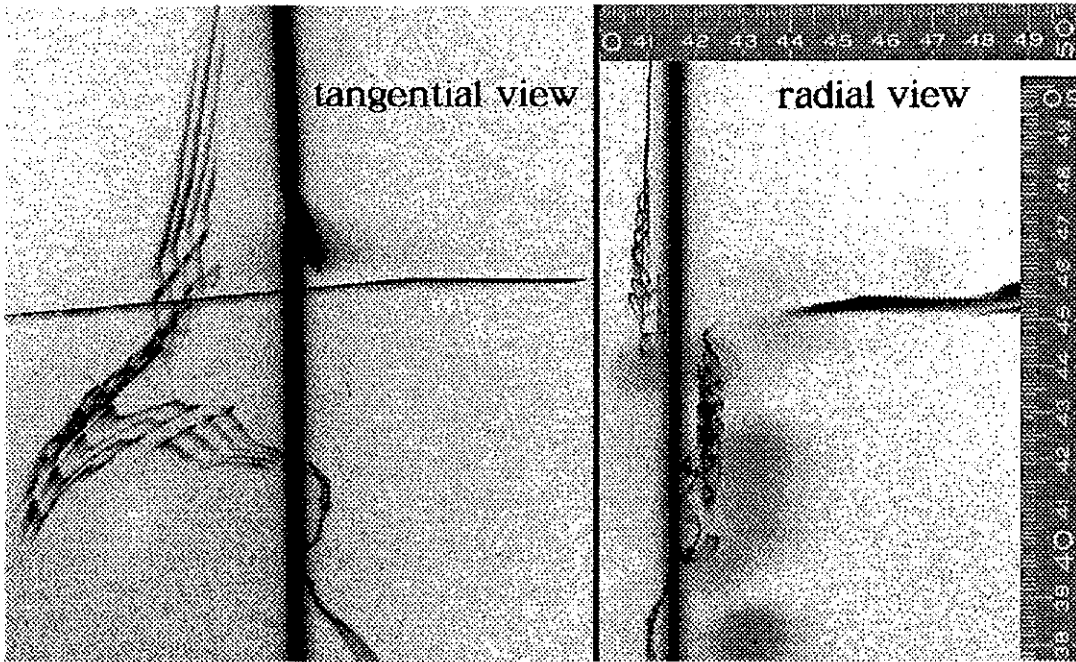


Fig. 10 Tangential view of the rotor flow showing the tip vortex of the preceding blade very shortly after the projection of the smoke line  
1 smoke line, 4 flash sequence

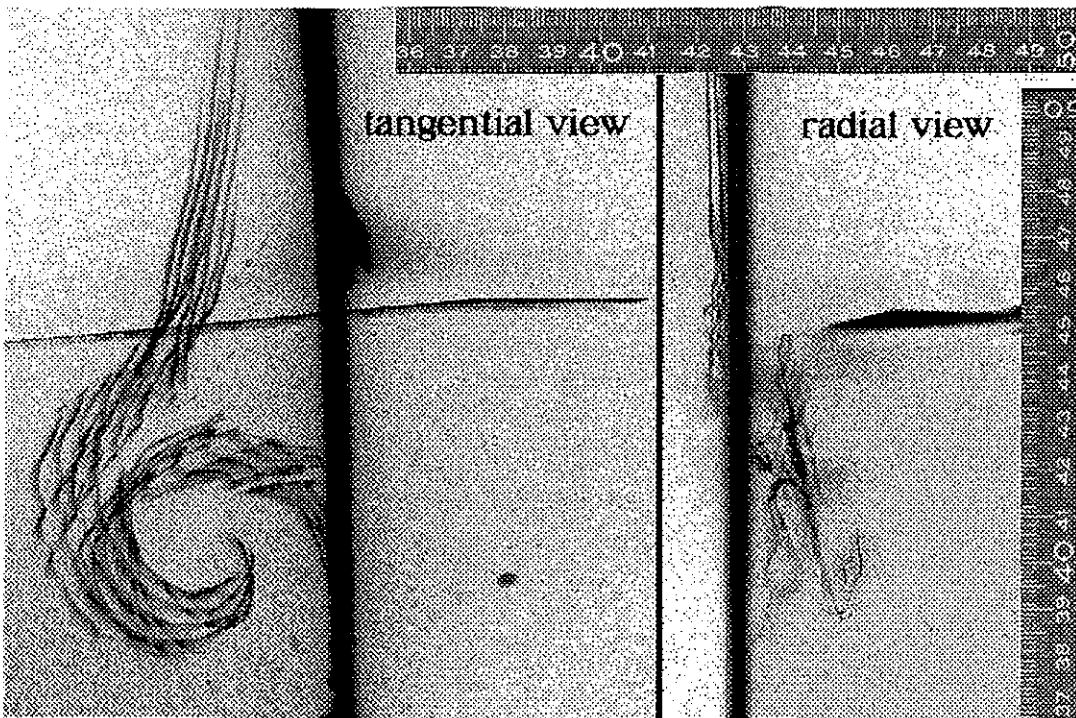


Fig. 11 Tangential view of the rotor flow showing the tip vortex of the preceding blade very shortly after the projection of the smoke line  
2 smoke lines, 4 flash sequence

As mentioned earlier, most photographs of this investigation have been taken at the lower tip speed of 53.5m/s using the 2-bladed rotor. This would provide the best chance to show the interesting flow near the swept back tip and a relatively undisturbed vortex at BVI with the following blade. A few experiments, however, have been performed using the 4-bladed rotor and/or full tip speed of 107m/s. Figure 13 gives an example with 4 blades at 53.5m/s tip speed. Here we find an extremely close encounter of the tip vortex with the following blade. It is obvious that this will produce a strong influence on the blade pressure slope and on the vortex structure itself. An interesting fact is that it was possible to depict the developing tip vortex and the tip vortex of the preceding blade at the same time with one smoke line only.

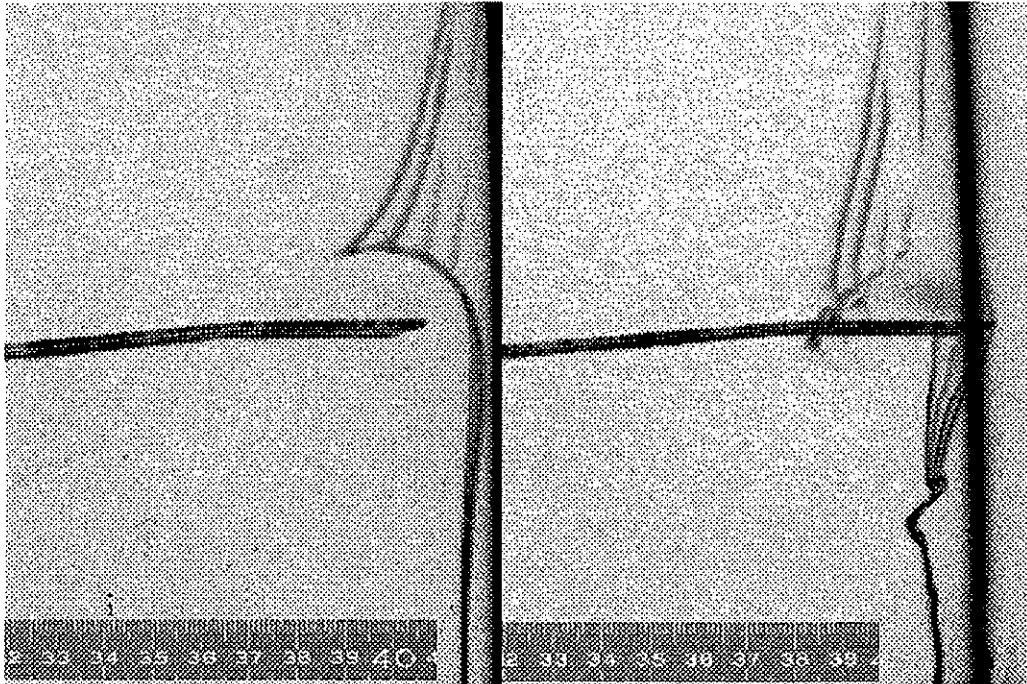


Fig. 12 Left: tangential view of the rotor flow at the very tip with developing tip vortex:  
The smoke line has been shot a little outside the rotor disk.  
Right: tangential view of the tip vortex development with a smoke line more  
inward to hit the vortex core more exactly. ( both pictures 1 smoke line, 4 flash sequence)

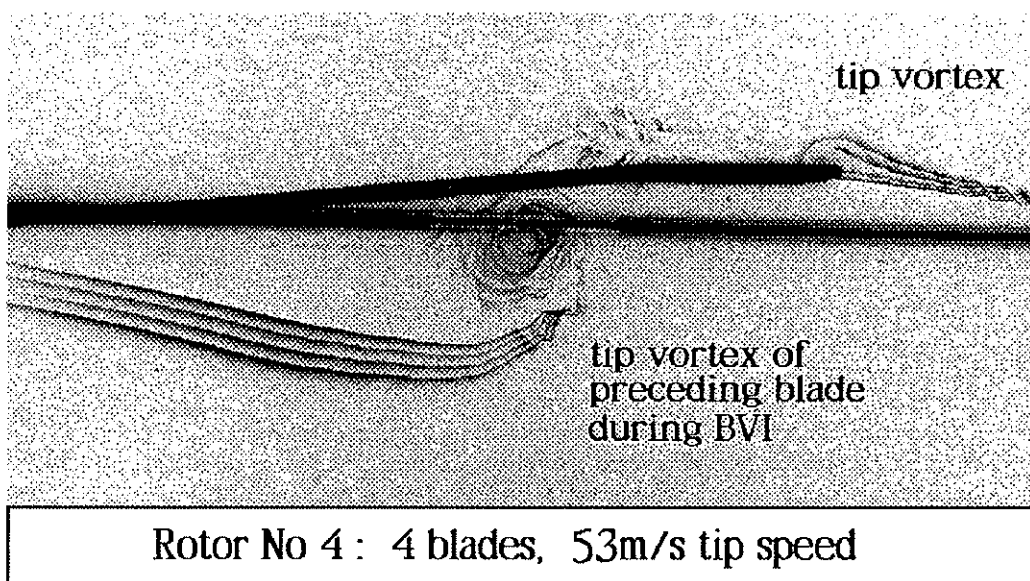


Fig. 13: Visualization of developing tip vortex and tip vortex of the preceding blade  
at the 4-bladed rotor. 1 smoke line, 4 flash sequence

Figures 14 and 15 show the flow at the high tip speed of 107m/s. For figure 14 the 2-bladed rotor was used, for figure 15 the 4-bladed rotor. These photographs give evidence that the FVG-technique works well at these relatively high flow speeds. However, the photographs had to be enhanced by using digital image processing because the contrast was too low. As the film sensitivity can not be improved over 25,000 ASA, it will be necessary to improve the light sources. Current energy of a single flash is about 15Ws, which could be extended by a factor of two.

A very important perception of all these photographs is the fact, that the novel Flow Visualization Gun technique provides the possibility to get information on single events or distinguished flow patterns at one instant. No averaging over time or interpolation over space is needed to measure the tangential velocities of a vortex during BVI or of a developing or newly forming tip vortex, if we manage to hit the vortex with the smoke trace at the right position into its core.

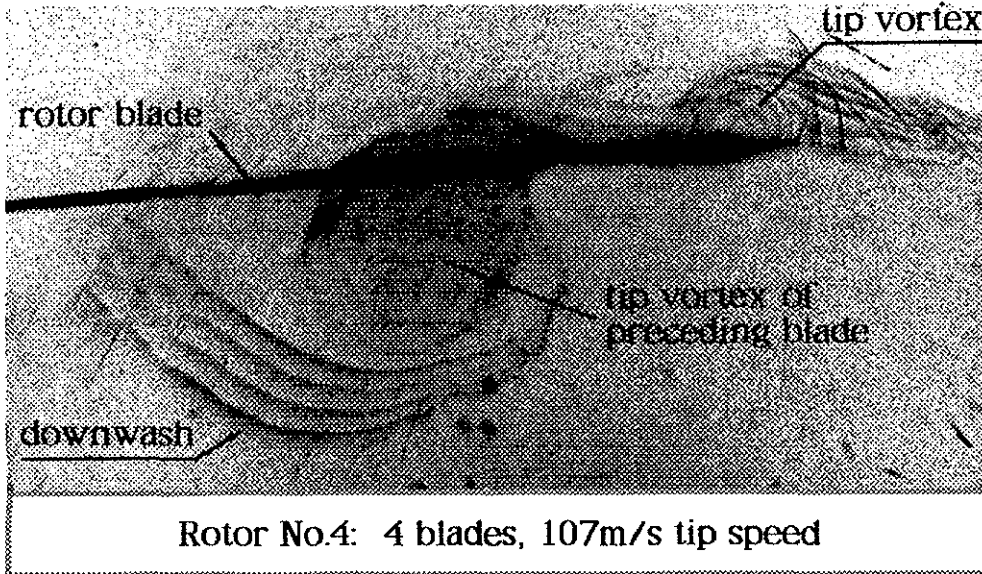


Fig. 14: Visualization of the developing tip vortex and the tip vortex of the preceding blade at the 4-bladed rotor at the full rotor tip speed of 107m/s. (1 smoke line, 4 flash sequence)

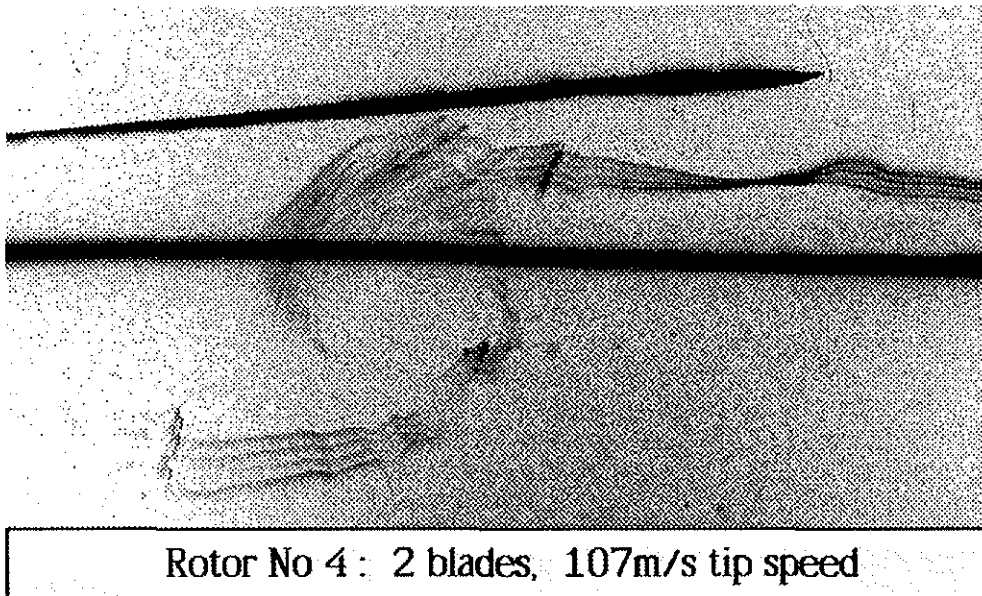


Fig. 15: Visualization of the tip vortex of the preceding blade at the 2-bladed rotor at the full rotor tip speed of 107m/s. (1 smoke line, 4 flash sequence)

## 6. RESULTS OF 3-DIMENSIONAL IMAGE ANALYSIS AND COMPARISON TO LDA DATA

Figure 16 shows the development of the tip vortex in a 3-dimensional view, which is reconstructed using a stereometric set of photographs. For this sketch the relations have been changed from the observer-fixed coordinate system to a blade-fixed coordinate system where the smoke line moves past the blade, shaped by the influence of the tip vortex. Streamlines are plotted, which connect the smoke line images.

The same technique was used for the view of the older tip vortex of the preceding blade in figure 17. In the very core of this vortex, however, the data are not exact. It is not possible to determine the paths of the smoke traces in the inner core of the vortex from photographs like figure 7, 8, or 9. To get more data in this region, more of the clearer photographs like figure 10 and 11 have to be vectorized. Figures 16 and 17 have been produced by using single stereometric sets of photographs only. To be able to plot the streamlines, the earlier mentioned little "irregularities" on the smoke lines have to be followed. This is easy at the location of the irregularities. Between them, a linear interpolation was used. It was assumed that, if there was an important flow pattern in between two recognizable irregularities, that we would see this pattern by its influence on the line. So, if there is no distortion or irregularity between two others, the flow must be clean and laminar in this region.

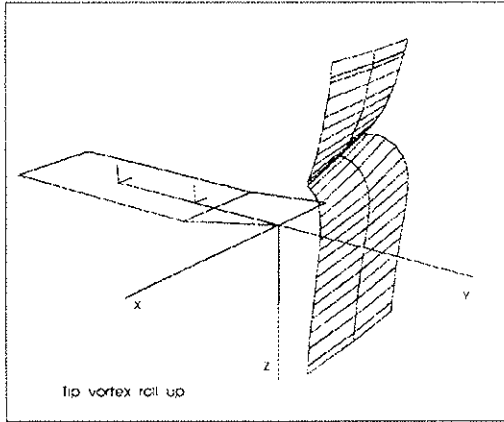


Fig. 16 Roll-up of the tip vortex and streamlines in a blade fixed coordinate system

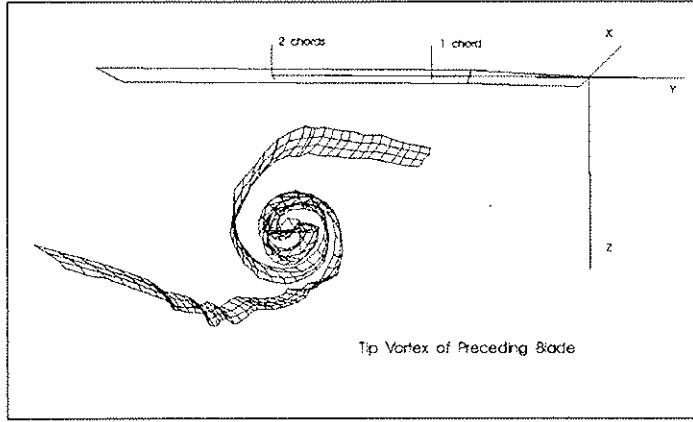


Fig. 17: Structure of the tip vortex of the preceding blade

After digitization and 3-dimensional vectorization of many photographs, a spatial interpolation in the complete tip region was possible. 16 sets of stereometric photographs were used for this interpolation. Using the interpolated data, streamlines can be placed anywhere in the tip region, for instance exactly cutting the vortex like figures 18 and 19, showing the vortex from different points of view.

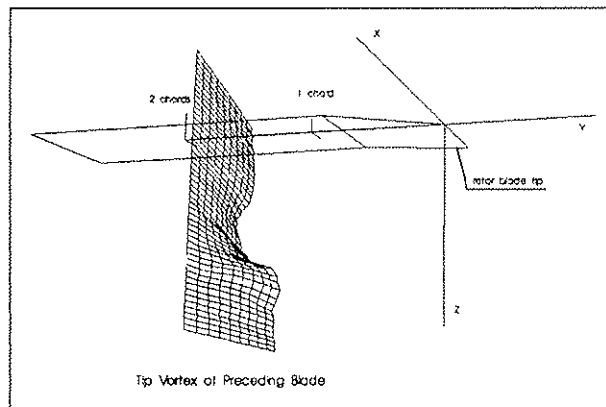
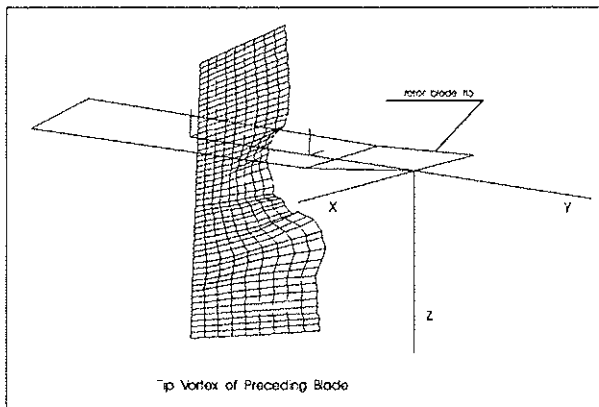


Fig. 18, 19: Streamlines in the tip vortex of the preceding blade after 3-D-interpolation

Additionally, it is possible to plot the complete velocity field in a 2-dimensional vector plot. Figure 20 shows the tangential velocities of the tip vortex and of the tip vortex of the preceding blade and the downwash velocities in the complete tip region at a plane near the trailing edge of the rotor blade. Figure 21 shows the corresponding vorticity contour plot. For this picture, the local rotation of the flow has been calculated. The iso-rotation-contours have a step size of  $200\text{s}^{-1}$ . Negative rotation has been plotted only. Clearly, the maximum of the vorticity for the newly developed tip vortex and for the older tip vortex of the preceding blade can be detected. Another local maximum of the vorticity near the start of the swept back tip indicates that there is a secondary vortex, induced by the special swept back tip geometry. More experiments in the future will provide the data necessary to determine whether this is a rolled-up secondary vortex or a distributed vorticity only. It is very important to examine the effect of this additional vorticity very thoroughly, because it can have a large influence on the circulation distribution of the rotor blade and therefore on the efficiency of the rotor. A velocity plot for a plane at one chord behind the trailing edge is shown in figure 22, together with the corresponding vorticity contour plot (fig. 23). If the two vorticity plots at the trailing edge and one chord behind the trailing edge are compared, the downward and inward movement of the vortices can be observed. The secondary vortex at the tip starts to turn around the stronger tip vortex. After about a quarter rotor turn this secondary vortex will merge into the tip vortex to form a relatively diffuse vortex causing lower pressure fluctuations on the blade at BVI. In ref. 14 this phenomenon has been examined more thoroughly using special 3-dimensional tip shapes.

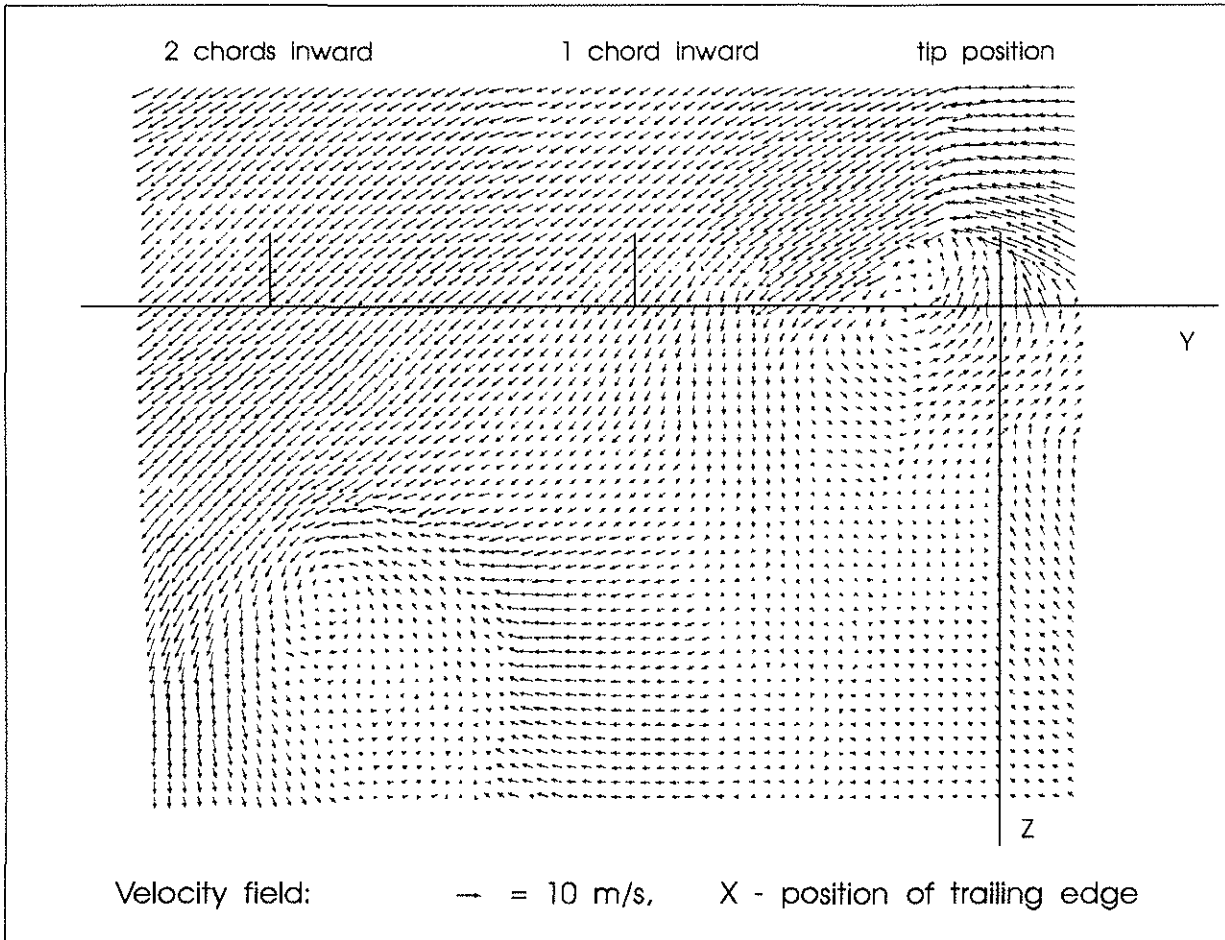


Fig. 20 Velocities in axial and radial direction (azimuthal position at trailing edge)

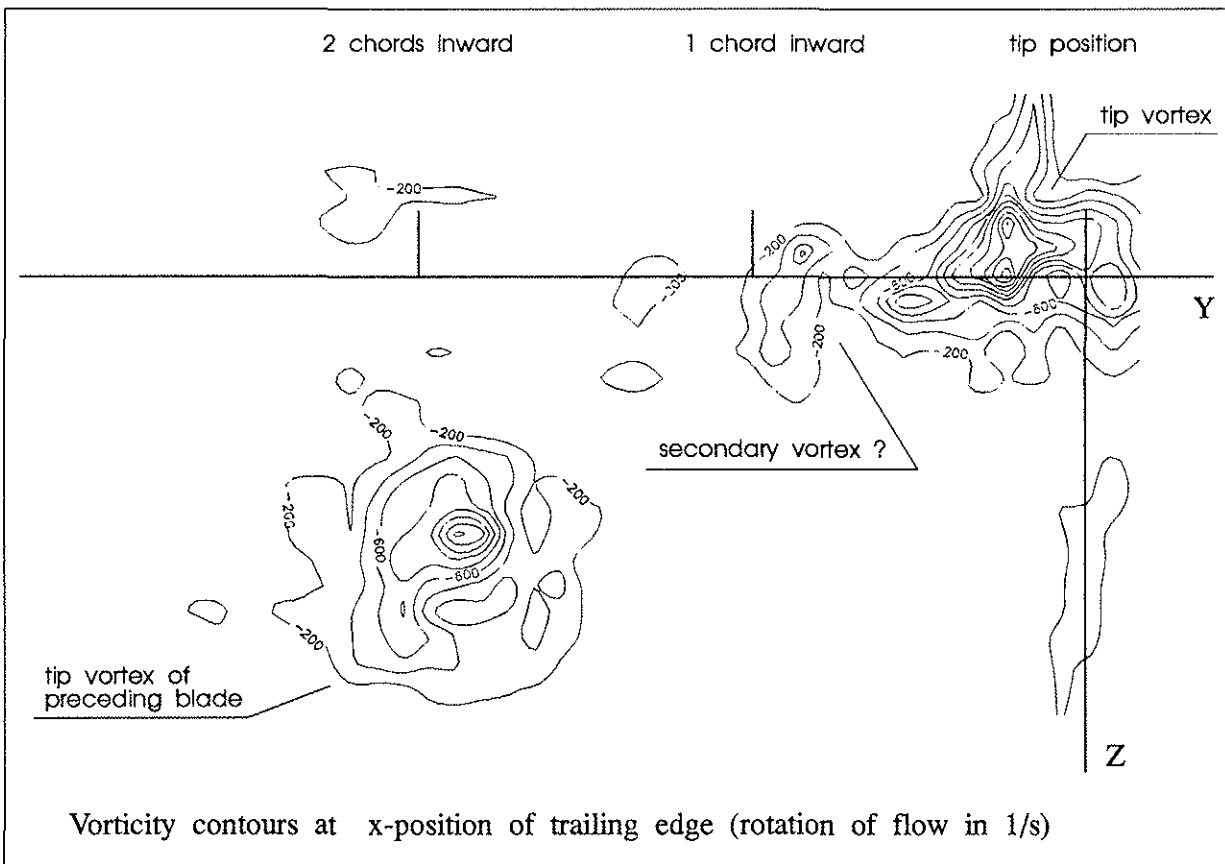


Fig. 21 Vorticity (rotation) contours (only negative rotation is plotted for clarity)  
 $(\omega_x = 1/2 * (\partial w / \partial y - \partial v / \partial z))$

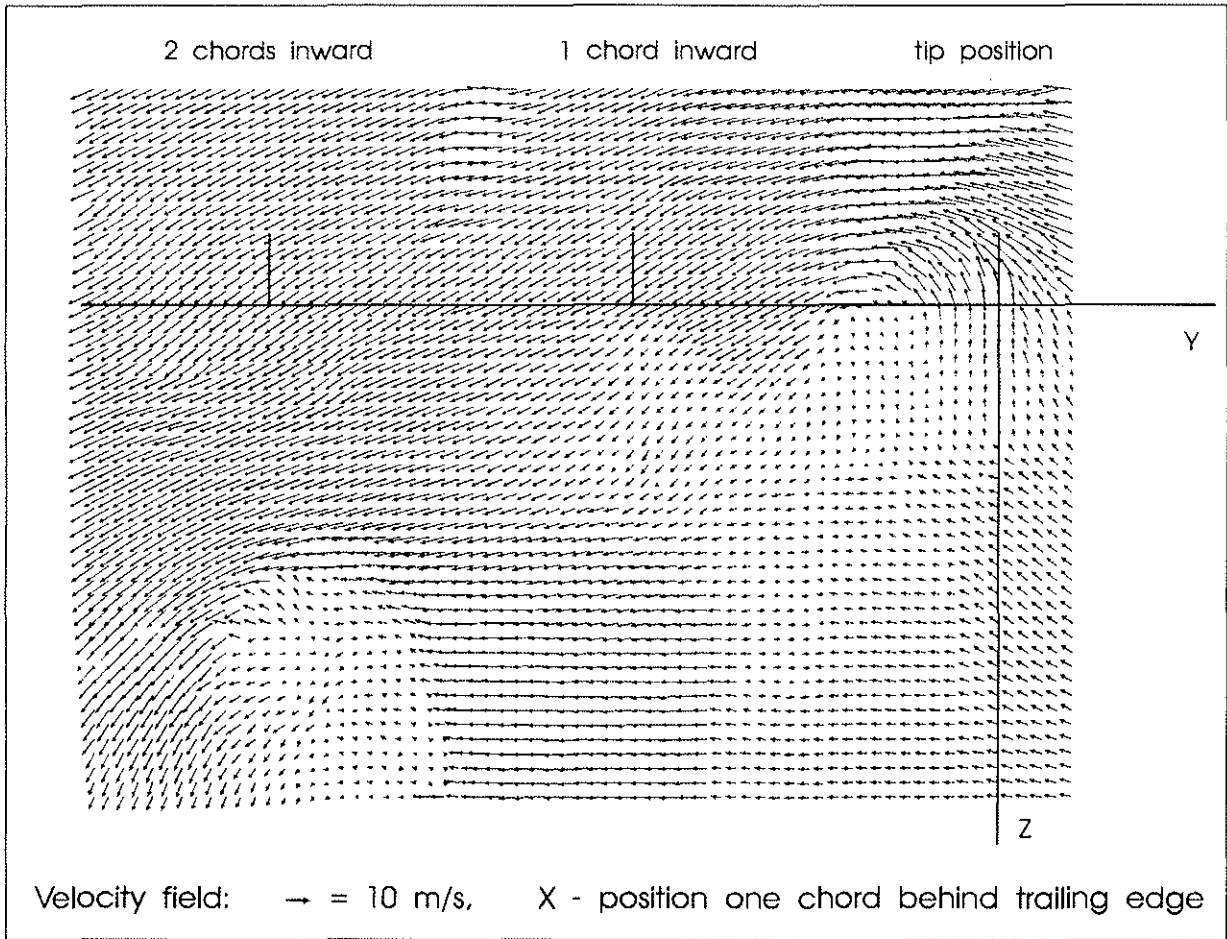


Fig. 22 Velocities in axial and radial direction (azimuthal position at 1 chord behind trailing edge)

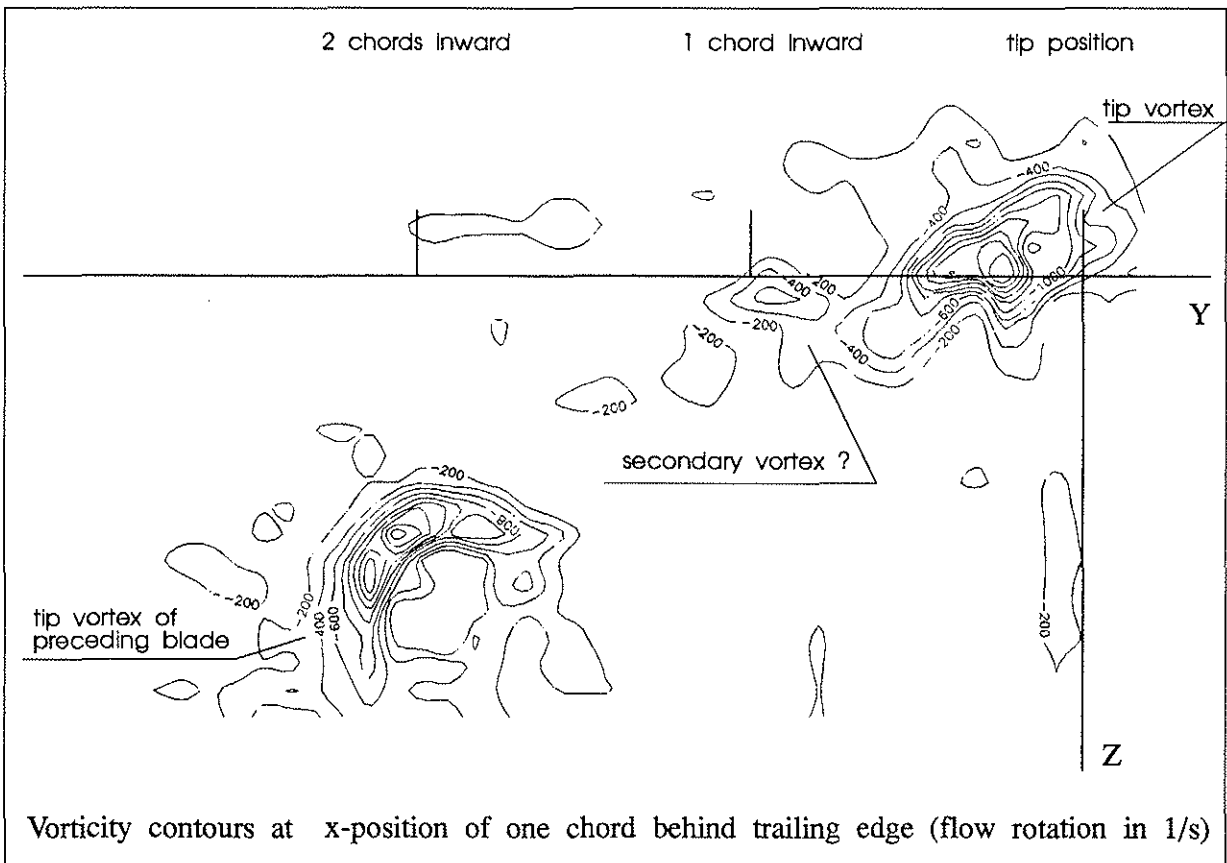


Fig. 23 Vorticity (rotation) contours (only negative rotation is plotted for clarity - contours all  $200\text{s}^{-1}$ )  
 $(\omega_x = 1/2 * (\partial w / \partial y - \partial v / \partial z))$

Even if the number of 16 stereometric smoke line images used for this interpolation is very small, the result looks reasonable good. Using more visualization images will improve the accuracy of the velocity field. For the inner core of the vortices there are no data from the visualization. To provide data in these regions, more experiments have to be performed to hit the vortex core exactly into its core at the exactly right timing.

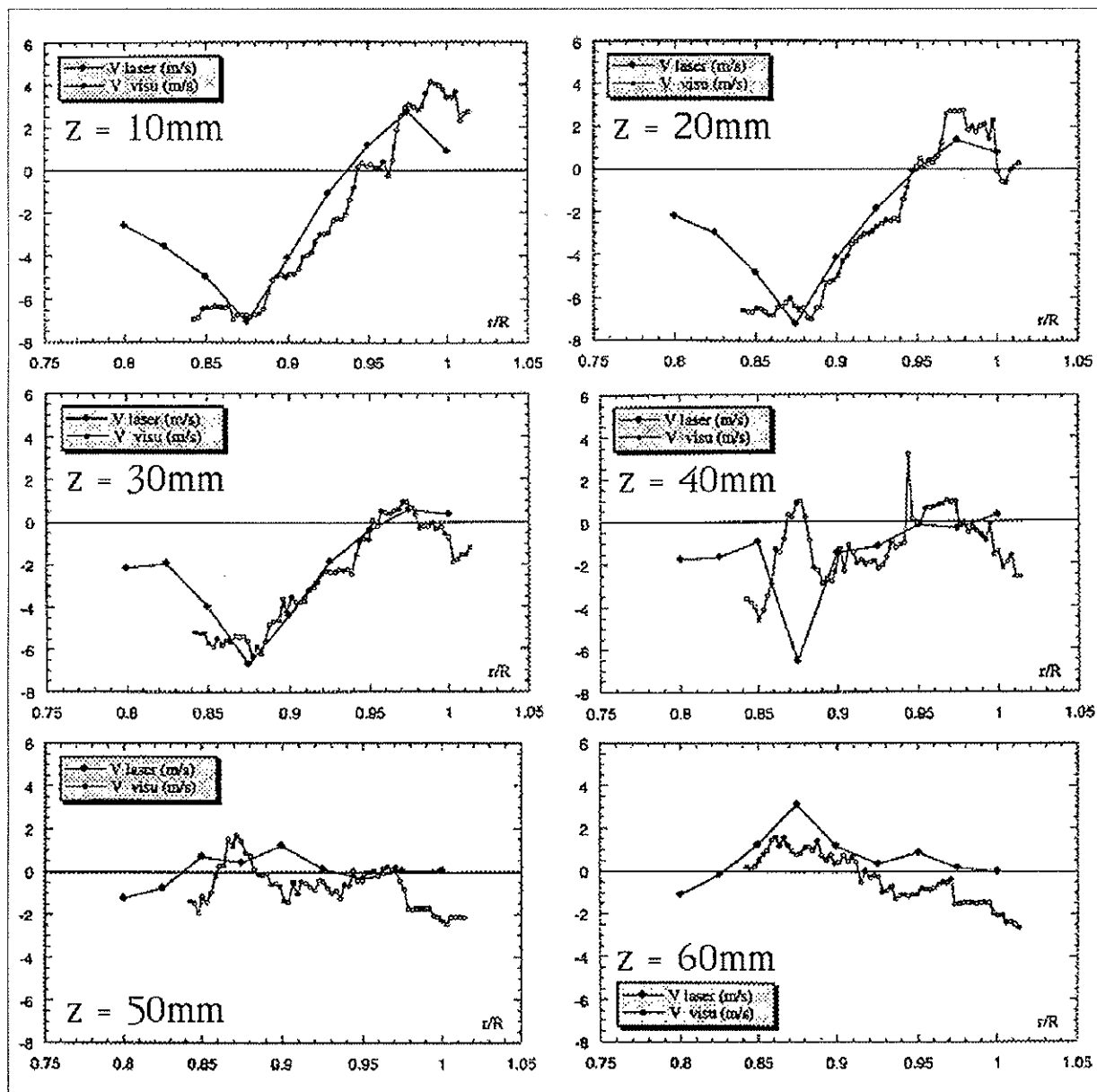


Fig. 24 Comparison of radial velocity for visualization and LDA at different vertical distance below the rotor disk ( $z=40\text{mm}$  is about the position of the vortex of the preceding blade) (coarse grid: Laser measurements | fine grid: FVG-smoke visualization measurements)

After the spatial interpolation of the flow field the data can easily be compared to the laser velocimetry data. Figure 24 shows the comparison of the radial velocities at the azimuthal position of the trailing edge in different vertical positions below the blade. Near to the blade the agreement is excellent, at the vertical position of the tip vortex of the preceding blade (about 40mm below the blade) there are some differences. These, however, can easily be explained by a slightly different vortex position in both experiments.

## 7. CONCLUSIONS

Using the Flow Visualization Gun technique it was possible to produce excellent pictures of the roll up patterns of the developing tip vortex and of the tip vortex of the preceding blade. Due to the dense white smoke and the sharp smoke lines the technique could be used even in the vortex core where the vortex had rolled up the smoke line several times. Turbulent flow patterns and shear layers can be recognized easily in the flow photographs. Therefore, the

technique is a perfect tool for the investigation of complex flow types. This is especially true if considering the reasonable good agreement of the quantitative data of the image analysis procedure compared to the laser velocimetry data. Some improvements of the technique may be necessary for the application at very high flow speeds (stronger light sources). It could be shown, however, that the tip speed of 107m/s, the regular tip speed for all investigations at IMFM, is not a problem for the method.

The rotor No 4 with its swept back tips is a very interesting configuration. Due to the special shape and its circulation distribution the developing tip vortex seems to be separated into a strong tip vortex and a weak secondary vortex. This will produce a different structure of the tip vortex after merging. As this will occur before the encounter with the following blade, the influence on the blade at BVI will be different. This is a very important fact which will be investigated more thoroughly in the future.

## 8. ACKNOWLEDGEMENT

Part of the flow visualization study has been supported by the CNRS by a "poste rouge" stipend. The experiments have been performed in the Institut de Mécanique des Fluides in Marseille, France. The image analysis has been performed partly at the IMFM and partly at the F.I.B.U.S. research institute in Düsseldorf, Germany. The authors are very grateful for the support by CNRS and the possibility to use the test facilities in both institutes. The authors would like to thank E. Aymard for his valuable help at all the experiments.

## 9. REFERENCES

1. Steinhoff, J. S., "A Simple Efficient Method for Flow Measurement and Visualization," Flow Visualization III, Hemisphere Publishing Corporation 1985) Springer-Verlag, Edited by W. J. Yang, pp. 19-24.
2. Müller, R.H.G. and Steinhoff, J. S., "Application of a New Visualization Method to Helicopter Rotor Flow," presented at the 8th AIAA Applied Aerodynamics Conference, Portland, Oregon, August 20-22, 1990.
3. Müller, R.H.G., "Eine neuartige Methode zur Visualisierung von Strömungen sowie Auswertung der Strömungsbilder mittels digitaler Bildverarbeitung," Abschlußbericht DFG (Deutsche Forschungsgemeinschaft) Mu802/1-1, 1990.
4. Müller, R.H.G., "Visualization and Measurement of Helicopter Rotor Flow Using Projected Smoke Filaments and Digital Image Processing," presented at the 16th European Rotorcraft Forum, Sept. 1990, Glasgow, Scotland.
5. Lorber, P.F., Stauter, R.C., Landgrebe, A.J., "A Comprehensive Hover Test of the Airloads and Airflow of an Extensively Instrumented Model Helicopter Rotor," Proceedings of the 45th AHS Annual Forum, May 1989.
6. Thomson, T.L., Kwon, O.J., Kemnitz, J.L., Komerath, N.M., Gray, R.B., "Tip Vortex Core Measurements on a Hovering Model Rotor," AIAA 25th Aerospace Sciences Meeting, Jan.12-15, 1987, Reno, Nevada.
7. Chace, William G., "Liquid Behavior of Exploding Wires," The Physics of Fluids, Vol. 2, No. 2, March-April 1959, pp. 230-235.
8. Scherrer, Victor E., "An Exploding Wire Hypervelocity Projector," Exploding Wires, Vol. 2, Plenum Press New York, 1962, pp. 235-244.
9. Bohn, J. L., Nadig, F. H., Simmons, W. F., "Acceleration of Small Particles by Means of Exploding Wires," Exploding Wires, Vol. 3, Plenum Press New York, 1964, pp. 330-351.
10. Lusseyran, D. and Rockwell, D., "Estimation of Velocity Eigenfunction and Vorticity Distributions from the Time Line Visualization Technique," Experiments in Fluids 6, pp 228-236 (1988).
11. Favier, D., Maresca, C. Berton, E., Plantin de Huges, P., "Investigation of the tip shape influence on the flowfield around hovering rotor blades," AIAA 22nd Fluid Dynamics, Plasma Dynamics and Laser Conference, Honolulu, June 1991
12. Silva, M. Favier, D. Ramos, J. Nsi Mba, M. Berton, E., "An Experimental Investigation of the Drag Mechanisms of a Helicopter Rotor in Hovering Flight," 19th European Rotorcraft Forum, September 14-16, 1993, Cernobbio (Como), Italy
13. Müller, R. H. G., Berton, E., Favier, D., Maresca, C., NSI MBA, M., "Experimental Investigation of the Flow Field Around Hovering Rotor Blade Tips," I.C.E.F.M. 94, Second International Conference on Experimental Fluid Mechanics, July 4-8, 1994, Torino, Italy
14. Müller, R. H. G., "Special Vortices at a Helicopter Rotor Blade," Journal of the American Helicopter Society, October 1990, pp 16-22